

Targeted Gene Transfer to Fetal Rat Lung Interstitium by Ultrasound-guided Intrapulmonary Injection

Tiago Henriques-Coelho^{1,2,4}, Sílvia Gonzaga^{1,3,4}, Masayuki Endo¹, Philip W Zoltick¹, Marcus Davey¹, Adelino F Leite-Moreira², Jorge Correia-Pinto³ and Alan W Flake¹

¹The Center for Fetal Research, Children's Hospital of Philadelphia, Philadelphia, Pennsylvania, USA; ²Department of Physiology, Faculty of Medicine, University of Porto, Porto, Portugal; ³Department of Development and Neophasia, Life and Health Sciences Research Institute (ICVS), School of Health Sciences, University of Minho, Braga, Portugal

In utero gene transfer to the developing lung may have clinical or research applications. In this study, we developed a new method for specifically targeting the fetal rat lung with adeno and lentiviral vectors encoding the enhanced green fluorescence protein (EGFP) marker gene at E15.5 using ultrasound biomicroscopy (UBM). Survival rate, morphometric parameters, viral biodistribution, and lung transduction efficiency were analyzed and compared to the intra-amniotic route of administration. Expression of EGFP started as early as 24 and 72 h after the injection of adenoviral and lentiviral vectors, respectively. Both vectors transduced lung parenchyma with gene expression limited to interstitial cells of the injected region, in contrast to intra-amniotic injection, which targeted the pulmonary epithelium. Expression of EGFP was most intense at E18.5 and E21.5 for adenoviral and lentiviral vectors, respectively. In contrast to lentivirus, adenoviral expression significantly declined until final analysis at 1 week of age. This study demonstrates the feasibility of targeting the fetal rat lung interstitium with viral vectors under UBM guidance during the pseudoglandular stage. This model system may facilitate *in vivo* studies of dynamic lung morphogenesis and could provide insight into the efficacy of prenatal gene transfer strategies for treatment of specific lung disorders.

Received 19 July 2006; accepted 23 October 2006.
doi:10.1038/sj.mt.6300057

INTRODUCTION

Prenatal gene transfer may offer a number of unique biological advantages relative to postnatal gene transfer.¹⁻⁴ The relatively high frequency and accessibility of stem cells and progenitors and their rapid proliferation in the fetus may offer efficiency advantages for stem-cell-targeted gene transfer. The low total

cell number in the fetus allows relatively high vector to target cell ratios, allowing the use of small amounts of vector. The immunologic immaturity of the early gestational fetus may induce tolerance to vector-associated or transgene-encoded proteins. Finally, *in utero* gene transfer has the potential to treat a disease before its clinical manifestations. Advances in prenatal diagnosis of genetic and congenital disorders with progressively more sensitive techniques may increase opportunities for consideration of prenatal gene therapy.^{5,6}

The fetal lung is an attractive target organ for fetal gene transfer. There are a number of genetic and acquired disorders with peri- or postnatal pulmonary manifestations. These include monogenetic diseases like cystic fibrosis⁷ or surfactant protein B (SP-B) deficiency that would presumably require long-term expression of the deficient or defective gene. However, there are also abnormalities of lung growth, such as congenital diaphragmatic hernia, or lung maturation, such as respiratory distress syndrome of prematurity, that could potentially benefit from strategies that achieve transient gene expression in specific pulmonary distributions. Additionally, an important advantage of the use of non-integrating viral vectors with transient gene expression is the avoidance of many of the current concerns regarding integrating vectors in the fetus, *i.e.*, insertional mutagenesis, developmental abnormalities, and germline alteration. We therefore anticipate the future need for a variety of lung-targeting strategies using different gene transfer technologies to achieve optimal therapeutic results.

In this study, we describe a new method for the direct injection of viral vectors into the rat fetal lung as early as the pseudoglandular phase of lung development. Using this technique, we assessed the efficiency and distribution of transduction in the lung, the biodistribution of transduction, and the toxicity of equine infectious anemia virus (EIAV) and adenovirus vectors expressing the enhanced green fluorescence protein (EGFP) marker gene after *in utero* injection. In addition, we compare the direct injection technique to intra-amniotic

Correspondence: Alan W Flake, Department of Surgery, Abramson Research Building, Room 1116B, 3615 Civic Center Boulevard, Philadelphia, Pennsylvania 19104-4318, USA. E-mail: flake@email.chop.edu

⁴These authors contributed equally to this work.

injection with respect to the efficiency of lung transduction, and organ, and cellular distribution.

RESULTS

The technique of ultrasound-guided injections

Ultrasound biomicroscopy (UBM) was used to scan the fetus to identify the lung (Figure 1). E15.5 was the earliest stage that we could perform *in utero* injections with a high survival rate and with accurate targeting of the developing lung. At E13.5 and E14.5, the lung bud was very difficult to visualize and mortality was unacceptably high. Important technical components of this procedure were the performance of a maternal laparotomy to expose the gravid uterus, and the application of pre-warmed sterile ultrasound gel over the uterus. This allowed manipulation of the fetal position into the axial orientation, which we found was the optimal plane for injection. The lung was best visualized between the level of the cardiac apex and upper part of the liver. Applying this imaging technique, we could inject small volumes (25–350 nL) of a viral vector suspension into the fetal lung parenchyma without any visually apparent injury to the lung or fetus. Injection of larger volumes was associated with the disruption of fetal lung architecture. The fetus and micropipette were manipulated so that the tip of the micropipette traversed only the uterine wall, amniotic membrane, amniotic cavity, fetal skin, and thoracic cavity (Figure 1 and Supplementary Video S1), avoiding the placenta, limbs, heart, or liver.

Safety of *in utero* gene transfer

Viral vectors used in this study were first-generation adenoviral vector and second-generation EIAV. To determine whether there was inherent toxicity from the viral preparation or from the early expression of the transgene, we compared survival after the intrapulmonary injection of viral vectors with injection of an equivalent volume of phosphate-buffered saline (PBS). The overall survival rate was 81 ± 6 , 82 ± 5 , and $87 \pm 4\%$ for the PBS, EIAV, and adeno groups, respectively. Survival rates were calculated per dam by the formula: (number of injected fetuses alive/total number of injected fetuses per dam) \times 100. There was no statistical difference among the groups at the studied time points (Table 1).

In total, 53 dams were used and 527 fetuses were injected. There were no maternal deaths. There was no evidence of

transplacental transfer of vector or transfected cells when maternal blood was analyzed for EGFP by flow cytometry (data not shown), although maternal tissues were not analyzed in detail. Fetuses delivered by cesarean section or at term were viable and without gross anomalies. Morphometric parameters, namely body weight, lung-to-body and heart-to-body weight ratios were similar and there were no statistical differences among the groups (Table 1). Macroscopic structure of the lung lobes, diaphragm, heart, and thoracic cavity was normal. Pups

Table 1 Survival and somatic growth

	PBS	EIAV	Adeno
<i>E16.5</i>			
Survival (%)	85 \pm 9	82 \pm 7	78 \pm 12
Body weight (g)	0.49 \pm 0.02	0.53 \pm 0.01	0.51 \pm 0.02
Lung weight (mg)	1.82 \pm 0.08	1.98 \pm 0.04	1.78 \pm 0.14
Heart weight (mg)	0.94 \pm 0.07	0.86 \pm 0.05	0.98 \pm 0.8
<i>E18.5</i>			
Survival (%)	94 \pm 5	87 \pm 6	89 \pm 1
Body weight (g)	1.60 \pm 0.04	1.74 \pm 0.10	1.52 \pm 0.09
Lung weight (mg)	3.19 \pm 0.10	3.27 \pm 0.12	3.23 \pm 0.12
Heart weight (mg)	0.75 \pm 0.04	0.62 \pm 0.02	0.72 \pm 0.05
<i>E21.5</i>			
Survival (%)	72 \pm 16	85 \pm 10	96 \pm 4
Body weight (g)	6.10 \pm 0.24	5.85 \pm 0.13	5.35 \pm 0.10
Lung weight (mg)	2.50 \pm 0.10	2.56 \pm 0.10	2.66 \pm 0.09
Heart weight (mg)	0.76 \pm 0.06	0.69 \pm 0.06	0.77 \pm 0.02
<i>P7</i>			
Survival (%)	72 \pm 11	82 \pm 12	82 \pm 7
Body weight (g)	15.19 \pm 0.13	14.00 \pm 0.68	16.43 \pm 0.64
Lung weight (mg)	2.26 \pm 0.05	2.15 \pm 0.08	2.29 \pm 0.06
Heart weight (mg)	0.67 \pm 0.01	0.76 \pm 0.02	0.70 \pm 0.02

EIAV, equine infectious anemia virus; PBS, phosphate-buffered saline. Survival is presented as mean \pm SE of survival rate per dam calculated by the formula: number of injected fetuses alive/total number of injected fetuses per dam \times 100.

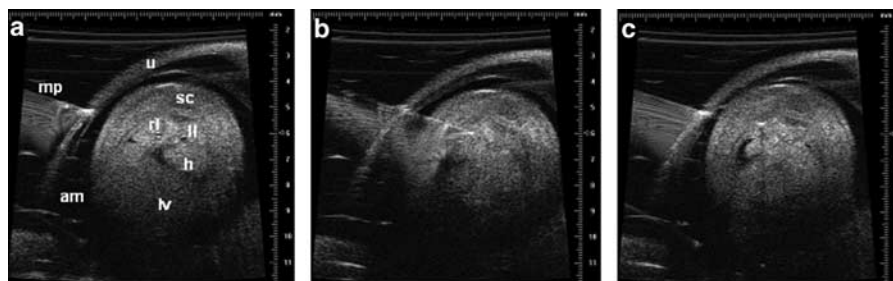


Figure 1 Fetal lung injections guided by UBM. (a) The micropipette (mp) is aligned to target the fetal right lung (rl). **(b)** The micropipette is advanced through uterine wall (u), and amniotic cavity (am) into the fetal lung; a small volume of viral vector suspension is injected into the pulmonary parenchyma. Other organs can be clearly visualized: heart (h), liver (lv), left lung (ll), and spinal cord (sc). **(c)** After injection, the micropipette is removed.

that survived until the seventh day after birth displayed overtly normal development and activity levels.

Efficiency of gene transfer to the lung and kinetics of gene expression

To determine the overall pattern of gene expression, we used stereoscopic fluorescence microscopy. After intrapulmonary injections, we observed that expression of EGFP, with the volumes of injectate utilized, was almost entirely limited to the injected lung and the ipsilateral pleural space after intrapulmonary injection (Table 2 and Figure 2). The time course of EGFP expression differed for the two vectors. EGFP expression was detected as early as 24 h after injection (E16.5) for adenoviral vector whereas the first expression did not appear until 72 h after injection for the EIAV-derived lentiviral vector (Figure 2). Maximum expression was observed at E16.5–E18.5 for adenovirus and at E21.5–P7 for lentivirus. For adenovirus, the intensity of lung EGFP fluorescence gradually decreased until P7 when it was barely discernable. For EIAV at P7, the intensity of the fluorescence was maintained, but the area of fluorescence was smaller presumably owing to the growth of the non-transduced lung and the relatively small area of initial transduction. In the adenoviral group, expression of EGFP was also seen in some fetuses in the skin and eyes, whereas in both groups the contralateral non-injected lung was positive in a few fetuses (Table 2).

Table 2 Viral vector biodistribution by fluorescence stereomicroscopy

	E16.5		E18.5		E21.5		P7	
	EIAV	Adeno	EIAV	Adeno	EIAV	Adeno	EIAV	Adeno
<i>n</i> injected	14	20	31	24	22	26	19	23
<i>Lung injected^a</i>								
–	7	1	2	1	1	0	1	0
+	5	1	18	3	11	11	5	12
++	1	8	8	10	8	13	10	10
+++	1	10	3	11	2	2	3	1
Lung non-injected	0	2	1	4	4	4	1	0
Brain	0	0	0	0	0	0	0	0
Diaphragm	0	0	0	0	0	0	0	0
Eye	0	6	0	5	0	9	0	2
Gonads	0	0	0	0	0	0	0	0
Heart	0	0	0	1	0	0	0	0
Intestine	0	0	0	0	0	0	0	0
Kidney	0	0	0	0	0	0	0	0
Liver	0	0	0	0	0	0	0	0
Muscle	0	0	0	0	0	0	0	0
Skin	0	2	0	3	0	4	1	0
Spleen	0	0	0	0	0	0	0	0
Stomach	0	0	0	0	0	0	0	0
Trachea	0	0	0	0	0	0	0	0

EGFP, enhanced green fluorescence protein; EIAV, equine infectious anemia virus. ^aNumbers represent the number of injected lungs that were negative or positive for EGFP fluorescence at the time points stated. Positive animals were subjectively ranked on a scale of + to +++ for intensity of fluorescence.

To confirm the fluorescence observations and to provide a better quantitative assessment of changes in gene expression over time in the injected lungs, we performed real-time polymerase chain reaction (PCR) (Figure 3a). Evaluation of the number of vector copies per lung revealed the presence of the vector at E16.5 in both EIAV and adenoviral groups. However, the number of vector copies was statistically higher for adenoviral vector at E16.5 and E18.5. Whereas adenoviral-associated copy number progressively decreased after E16.5, copy number from EIAV gene transfer increased after E18.5 and was statistically greater than adenovirus at P7. It is important to note that this is not a direct comparison of transduction efficiency between the two viral vectors owing to the differing volumes and titers injected. Approximately 25 nL of adenoviral vector at a titer of $2-8 \times 10^{11}$ i.p./mL was injected versus 350 nL of EIAV vector at a titer of 10^8-10^9 i.p./mL. Thus, even at the extremes of volume allowed by the model, there was at least a 100-fold greater dose of adenoviral vector injected. However, this quantitative data confirm the fluorescence observation of the rapid diminution in EGFP expression for adenoviral-transduced lungs over the interval between E16.5 and P7. In contrast, copy numbers, although relatively low, were maintained in the EIAV group throughout the duration of the study.

Biodistribution of viral vectors

To confirm our impression that EGFP gene expression was relatively limited to the lung after intraparenchymal injection and to more globally assessed gene expression in the injected fetuses, we performed quantitative PCR on several tissues at E21.5 (Figure 3b). A statistically higher number of vector copies relative to PBS controls were observed in the heart and in the tract of the micropipette through the thoracic wall in both the EIAV-EGFP and Adeno-EGFP groups. For all other tissues analyzed, there were no statistical differences in EGFP expression above the PBS-injected controls.

Cellular distribution of gene transduction within the lung

EGFP-positive cells were predominantly found in the pulmonary interstitium for both the EIAV and adenoviral groups, after intrapulmonary injections (Figure 2i–p). There was no expression of reporter gene in the surface epithelium of airways or in the vascular endothelium. EGFP-positive cells neither stained for vimentin, a mesenchymal-derived cell marker (Figure 4a and b), nor for SP-B, a surfactant protein expressed in Type II pneumocytes (Figure 4c and d and Supplementary Figure S2). Therefore, we demonstrated that transduced cells were located within the interstitial compartment of the lung and that they were not epithelial. This is in distinct contrast to the epithelial-restricted expression seen with intra-amniotic vector injections (Figure 4e and f).

DISCUSSION

We report for the first time, the feasibility of using UBM to perform *in utero* intrapulmonary injections in rats at the pseudoglandular stage of lung development. Both adenoviral and lentiviral vectors efficiently transduced lung parenchyma, although different expression patterns were observed following

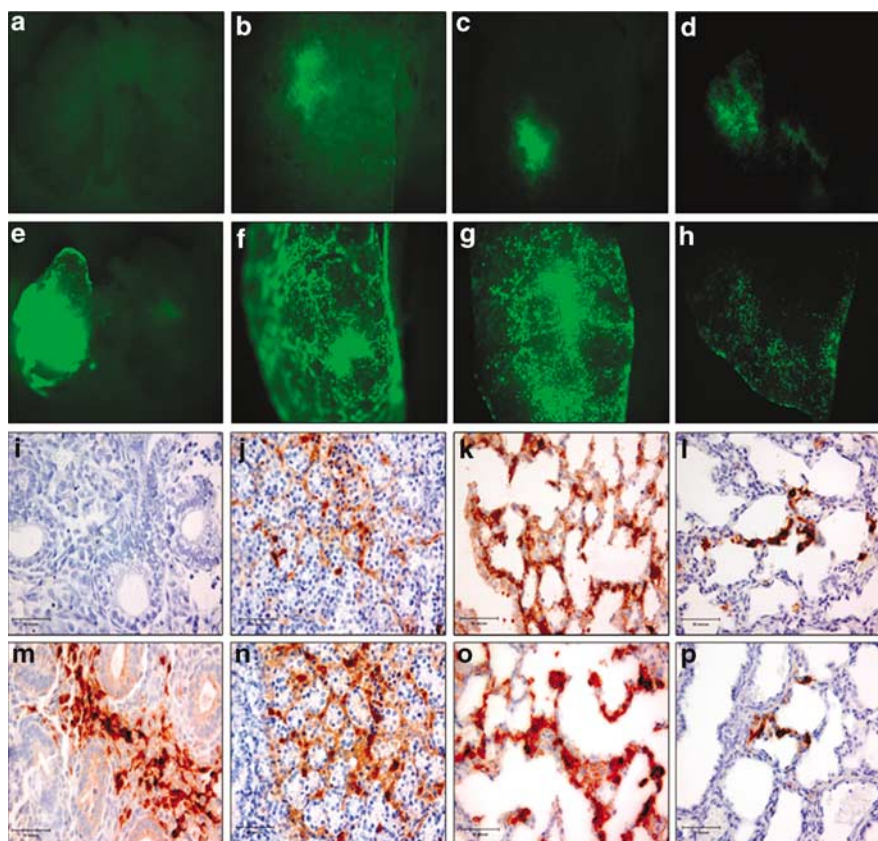


Figure 2 Fluorescence stereomicroscopy and lung immunostaining for EGFP. Injected fetuses at E15.5 were analyzed at E16.5, E18.5, E21.5, and P7. Representative examples of fluorescence stereomicroscopy of the lungs at each analysis time after injection with (a-d) lentiviral vector and (e-h) adenoviral vector are shown. Viral vector transduction can be detected by green fluorescence in an area around the location of the injection. Representative images of immunostaining for EGFP from the lungs injected with (i-l) lentiviral vector and (m-p) adenoviral vector at the same analysis times are presented. (i-l) Lentiviral vector was only detected at (j) E18.5, with more EGFP expression being detected at (k) E21.5 and maintained until (l) P7. (m-p) Adenoviral vector induced an earlier expression of EGFP with maximal expression at (m, n) E16.5-E18.5. EGFP expression was analyzed by immunoperoxidase (brown staining) and both vectors were expressed in interstitial cells. No epithelial expression was detected. Bar = 50 μ m.

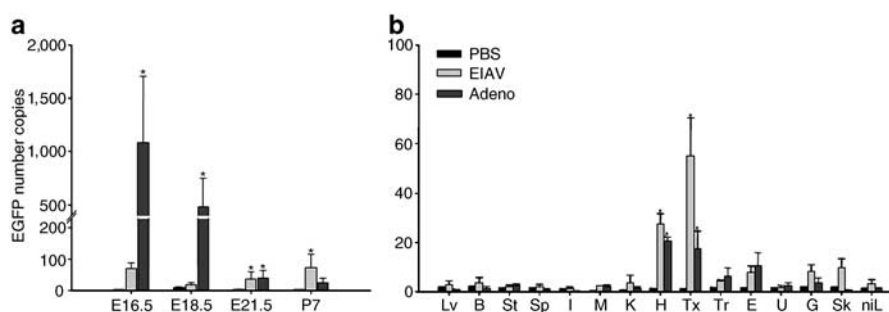


Figure 3 Quantitative PCR for EGFP. (a) Number of vector copies detected by quantitative PCR in lung samples after PBS, adenoviral, and lentiviral injections, at different time points of gestation. (b) Number of vector copies detected by quantitative PCR in non-pulmonary tissues and non-injected lung samples after PBS, adenoviral, and lentiviral injections at E21.5. Lv, liver; B, brain; St, stomach; Sp, spleen; I, intestine; M, muscle; K, kidney; H, heart; Tx, thorax; Tr, trachea; D, diaphragm; E, eye; G, gonads; Sk, skin; niL, non-injected lung of injected fetuses. *Significant differences = $P \leq 0.05$ compared to PBS control.

injection. As expected, adenoviral vector expression appeared quickly and was transient, whereas lentiviral vector expression was relatively delayed and persisted through the time period of this study. Unexpectedly, in contrast to intra-amniotic injections, both vectors selectively transduced interstitial cells and not alveolar or airway epithelial cells, or vascular endothelial cells.

Several routes of vector administration have been utilized to achieve prenatal gene transfer to the lung including intra-amniotic,⁸⁻¹¹ systemic,¹²⁻¹⁴ intratracheal,¹⁵⁻¹⁷ and intrapulmonary.^{18,19} Intra-amniotic and systemic approaches share the same limitations of being nonspecific for fetal lung. Intratracheal and intrapulmonary delivery, although more specific to the lung,

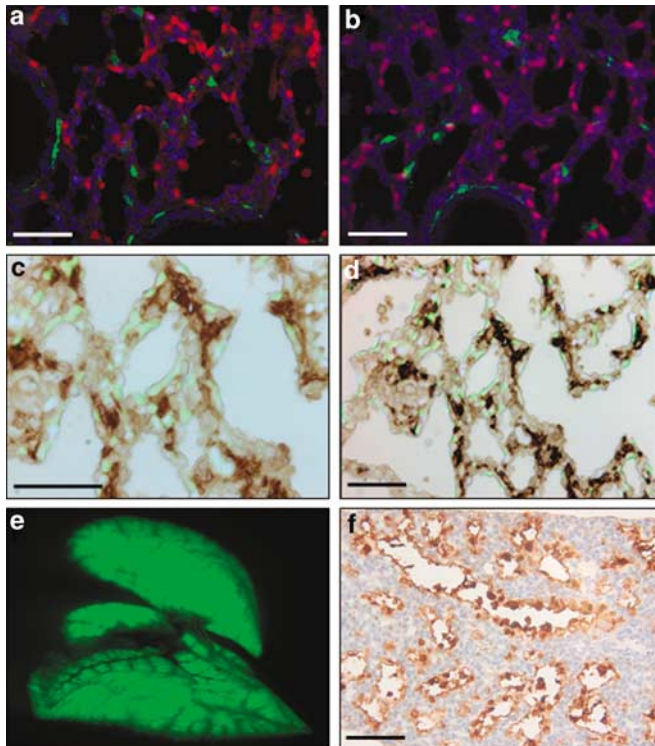


Figure 4 Interstitial localization of transduced cells after intraparenchymal injection. **(a, b)** Lung double immunofluorescence for EGFP (green) and vimentin (red) in fetuses injected with **(a)** lentiviral and **(b)** adenoviral vectors. Lungs were harvested at P7. **(c, d)** Lung immunoperoxidase staining for EGFP (brown) and immunofluorescence for SP-B (green). Images represent an overlay of bright light and fluorescent images at original magnification $\times 60$ and $\times 40$ for **c** and **d**, respectively. Merged images were created with Adobe Photoshop software and adjusted for brightness, contrast, and opacification to allow optimal visualization of both markers (original images before manipulation can be seen in **Supplementary Figure S2**). EGFP-positive cells did not colocalize with vimentin, or SP-B, and were localized within the interstitial region of the parenchyma. **(e, f)** Epithelial localization of transduced cells after intra-amniotic injection. Intra-amniotic injections were performed at E16.5 and the fetuses were harvested at E21.5. **(e)** Fluorescence stereomicroscopy and **(f)** lung immunostaining for EGFP are presented demonstrating the transduction of only epithelial cells. Bar = 50 μm .

have previously only been performed in large animal models. Tarantal *et al.*¹⁸ demonstrated, in a non-human primate model, that intrapulmonary injections during the pseudoglandular stage allowed specific targeting of the lung relative to injections performed during the embryonic stage. In this study, we used UBM to perform *in utero* intrapulmonary injections. The use of this relatively new imaging technology made injection of the fetal rat lung at E15.5. UBM utilizes high-frequency (20–100 MHz), pulse-echo ultrasound for imaging live tissues and organs, allowing near microscopic resolution and has been previously utilized for fetal brain injections.^{20,21} Using UBM, we could successfully target the rat lung during the mid-point of the pseudoglandular stage of lung development with a high fetal survival rate.

First-generation adenovirus and EIAV lentivirus-based vectors were used in this study. We chose to study first-generation adenoviral vectors rather than adeno-associated viral vectors

because we wished to see rapid, high-level expression of the marker gene. We used EIAV owing to the fact that human immunodeficiency virus-1-based lentiviral vectors have not shown high efficiency transduction^{22,23} in many tissues and owing to the successful application of EIAV vectors in fetal rodent models by Waddington *et al.*¹⁴ Adenovirus has been one of the most extensively studied recombinant viral systems because of its high transduction efficiency, rapid expression, accommodation of large transgene inserts, and high titers.^{23–26} The primary problem with adenovirus is its high immunogenicity and propensity to invoke strong immune responses. We previously documented that this is a problem with intratracheal administration in late gestational fetal lambs; however, in the same model, no significant inflammation is observed with adenoviral administration during the preimmune phase of lamb immunologic development.²⁷ Similarly, as we would predict from the stage of rat immune development at E15.5, we saw no overt inflammatory response in the lung by histology in these experiments. However, as the purpose of this study was not induction of immune tolerance, we did not perform a detailed analysis of immune response to adenoviral products or transgene. In contrast to adenovirus, lentiviral vectors are relatively non-toxic and minimally immunogenic and can stably integrate transgene into dividing and non-dividing cells with subsequent long-term gene expression.^{28–30} The main disadvantages are the low titers that are usually obtained *in vitro*.²³ This proved somewhat limiting in the current study. With EIAV vector titers of only 10^7 – 10^8 infectious particles per mL, we needed to inject the maximal tolerated volume of 350 nL of EIAV to achieve significant transduction.

The rapid loss of EGFP expression in the adenoviral-transduced lungs is in keeping with the known episomal location of adenoviral gene expression, the small volume of vector administered (25 nL), and the rapid proliferation of fetal lung tissue. Our data are also consistent with the known capacity of EIAV to stably integrate transgene into the host genome. In the EIAV-transduced lungs, there was, if anything, a slight increase in copy number at P7. We would conclude from this analysis that adenovirus would be the most appropriate vector to use when the goal is to induce rapid and transient overexpression of a gene in this model, whereas, lentivirus would be a more suitable vector to induce sustained and long-term gene expression.

Gene transfer was localized to the injected lung with the only exceptions being the needle track through the thorax and a very low copy number in the heart. This could be due to inadvertent injection of the heart but is more likely due to the small amount of intravascular injection associated with this technique. A few animals had EGFP expression noted by stereoscopic fluorescent analysis in the skin or eye. However, in the animals selected for PCR analysis, these tissues did not have statistically higher gene copy numbers than PBS controls. This discrepancy likely represents inconsistent amounts of leakage of the vector into the amniotic space during removal of the micropipette. The lack of pulmonary epithelial transduction in these animals despite intra-amniotic leakage is most likely explained by the very minimal volume of leakage into the amniotic space relative to the volume of injectate in the intra-amniotic injection

experiments as well as the timing of the injection. In our experience, and that of others,⁸ efficient transduction efficiency of pulmonary epithelium after the intra-amniotic delivery of vector is limited to a narrow gestational window related to the onset of fetal respiratory movements. In this study, intrapulmonary injections were performed 1 day before the time point when efficient transduction to pulmonary epithelium is seen after intra-amniotic injection.

One of the most interesting findings in our study was the specificity for the interstitial compartment seen with both the vectors utilized. There was no expression of reporter gene in the surface epithelium of airways or in the vascular endothelium. The obvious question is, what population of cells was transduced? Unfortunately, we were not able to definitively identify the cells in this study owing to a lack of specific markers for cell types in the interstitium. Although we suspected that the cells were mesenchymal in origin, they do not stain with vimentin, a common mesenchymal and fibroblast marker. Attempts to colocalize EGFP staining with SP-B, a surfactant protein expressed in Type II pneumocytes, confirmed that the transduced cells were not epithelial, and that they were located within the interstitial compartment of the lung. This is in distinct contrast to the epithelial restricted expression seen with intra-amniotic vector injections. Although the obvious explanation is the route of injection, the needle tip must traverse all layers of lung parenchyma on insertion and withdrawal and one would expect to see epithelial transduction as well. We do not have an explanation for this observation but it was seen consistent in all lungs examined and with both vectors utilized. In contrast, in the two previous studies of direct lung transduction in primates using human immunodeficiency virus-1 lentiviral vectors,¹⁸⁻¹⁹ only epithelial expression was described, so this appears to be a model-dependent observation. Further characterization of the type of cells that were transduced will require additional studies. Nevertheless, to our knowledge, this is the first observation of this pattern of parenchymal expression with any reports of prenatal lung gene transfer. The observation of transduction of distinct cell populations within the lung with different routes of transduction raises the possibility of manipulating gene expression in specific and separate cell populations within the developing lung. This may have interesting applications toward understanding mesenchymal epithelial inductive interactions during the pseudoglandular phase of lung development.

The ability to achieve gene transfer by direct intrapulmonary injection in a rat model provides a novel tool for the exploration of potential therapeutic strategies for lung disorders and for biological studies examining the effects of specific genes on lung development. Obvious advantages of this technique include ease of manipulation, minimal expense, and, if translatable to the mouse, the availability of well-characterized murine models of human lung diseases.³¹⁻³³ Although this study was performed in rats, we now also have preliminary experience with this approach in murine fetuses with similar success (data not shown). Finally, the possibility of targeting the lung during the pseudoglandular stage may present unique experimental and, ultimately perhaps, clinical opportunities. This stage, characterized by intense

branching morphogenesis, is the period of greatest overall growth of the airways and vasculature of the fetal lung, and corresponds to a stage of immunologic immaturity and thymic processing of self-antigen. Therefore, gene transfer during this period has the potential to have major effects on the key elements of lung growth with minimal potential for detrimental immune responses.

MATERIALS AND METHODS

All experimental protocols were approved by the Institutional Animal Care and Use Committee at the Children's Hospital of Philadelphia and followed guidelines set forth in the *National Institutes of Health Guide for the Care and Use of Laboratory Animals*.

Viral vector preparation. EIAV-derived lentivirus vector expresses the EGFP reporter gene from an internal cytomegalovirus immediate-early promoter. The packaging plasmid, pEV53, and the SIN EIAV transfer vector^{34,35} were kindly provided by Dr Bruce A Bunnell (Tulane University, New Orleans, LA). The plasmid pFL85, containing the EIAV provirus,³⁶ was kindly provided by Dr Robert Stephens (National Cancer Institute, Frederick, MD). The transfer plasmid, pZEK-CMV-*eGFP*, was reassembled retaining the left and right long terminal repeats and the extended packaging was inserted after the left long terminal repeat.³⁷ All Woodchuck hepatitis virus sequences were removed and replaced with the modified Woodchuck hepatitis post-transcriptional regulatory element.³⁸ Viral vector pseudotyped with the vesicular stomatitis virus G-protein (VSV-G) envelope was generated by three plasmid co-transfections in 293T cells as described previously.²⁹ The initial transfection conditions were: 18 μ g pE2KEGFP + 18 μ g CMV Δ R8.91 + 12 μ g VSV-G + 96.9 μ L 2 M CaCl₂ + 2.5 mM HEPES, pH 7.3 up to a total volume of 780 μ L added to 780 μ L of 2 \times HEPES buffer solution (HeBS) (280 mM NaCl, 50 mM HEPES, 1.5 mM Na₂HPO₄, pH 7.0). The lentivirus vector supernatants were concentrated by ultracentrifugation at 28,000 r.p.m. for 90 min at 4°C (SW-28 rotor, Beckman, Palo Alto, CA). Titers were determined by plaque-forming assay. Vector particle titers obtained range from approximately 1×10^8 to 1×10^9 infectious particles per mL.

The *E1-E3* replication-deficient recombinant adenovirus, based on human serotype 5, contains *eGFP* under the human cytomegalovirus immediate-early promoter (rAd-CMV-*eGFP*) and was obtained from the vector core facility of the Gene Therapy Program (Division of Medical Genetics, University of Pennsylvania, Philadelphia, PA).¹³ Recombinant vectors were prepared as previously reported.³⁹⁻⁴¹ Adenoviral vector was stored at -80°C in PBS with 5% glycerol. Before administration, vector aliquots were resuspended in fresh PBS at a concentration of $2-8 \times 10^{11}$ infectious particles per mL.

Viral vectors administration. Ultrasound-guided injections. Time-dated pregnant Sprague-Dawley rats (Charles-River, Wilmington, MA) at 15.5 days *post coitum* (E15.5) were anesthetized with isoflurane (3.5% for induction, 2% for maintenance) and laid supine on a platform. The body temperature was monitored via a rectal probe (Indus Instruments, Houston, TX) and maintained at 36-38°C. The surgical site was chemically depilated and disinfected. A 2-cm ventral midline incision was made and the uterus containing one or two fetuses was partially exposed and covered with a pre-warmed sterile ultrasound gel (Aquasonic, Parker Laboratories, Fairfield, NJ). Fetuses were positioned to obtain axial views of the lungs in B-mode using a 40 MHz probe (VisualSonics Vevo 660, Toronto, Canada). Glass microcapillary pipettes (outer diameter 1.14 mm, inner diameter 0.53 mm, Humagen, Marlton, NJ) were backfilled with mineral oil (Sigma, St Louis, MO), connected to the micropipette holder that was attached to a three-axis microinjector unit (VisualSonics Vevo 660), filled with the PBS or viral vector

suspension (5 μ L), and aligned with the scanhead. Under two-dimensional imaging, the micropipette tip was physically advanced through the uterine wall and amniotic cavity into the lung and a specific volume was injected. The micropipette was then physically retracted and the next fetus was positioned and the procedure was repeated. Between six and 10 fetuses were injected per dam. The maximum time of the surgical procedure (between maternal abdominal incision and its closure) was 60 min. The abdomen was closed and dams recovered in a warming chamber. Fetuses were harvested at E16.5, E18.5, E21.5 (by cesarean), and P7. Fetuses or pups were inspected for the presence of macroscopic abnormalities and body, wet lung, and heart weights were recorded. Tissue samples were collected for histological and PCR analysis.

Intra-amniotic microinjections. Time-dated pregnant Sprague–Dawley rats (Charles-River, Wilmington, MA) at 16.5 days *post coitum* (E16.5) were anesthetized as described above. A midline laparotomy was made and one horn of the uterus was exposed at a time. The injections were performed under direct vision with glass microcapillary pipettes connected to a microinjector. Pipettes were backfilled with adenovirus suspension and 5 μ L were injected into the intra-amniotic cavity of each fetus. Maximum time of the surgical procedure was 20 min. After injections, the abdomen was closed in two layers and dams recovered in a warming chamber. Fetuses were harvested at E21.5 (by cesarean) and lungs were collected for analysis.

Fluorescence stereomicroscopy. Injected fetuses were visualized under fluorescence stereomicroscopy (MZ16FA, Leica, Heerburgg, Switzerland) immediately after harvesting, to evaluate EGFP expression, transduction efficiency, and biodistribution of the vector. After removal of the fetus from the amniotic sac, the eyes and skin were inspected for fluorescence. Thoracotomy was performed and the heart and lungs were visualized. The liver, spleen, stomach, intestines, kidneys gonads, brain, and muscles of the lower limbs were also inspected.

Histology and immunohistochemistry. Tissue specimens collected for histology and immunohistochemistry were fixed in 10% buffered formalin, embedded in paraffin, and stained with hematoxylin and eosin. To evaluate and localize EGFP protein in the harvested lungs, 4 μ m serial sections were rehydrated and placed in 1% sodium borohydride in PBS. Slides were blocked for specific protein with goat serum (1:10 dilution) and incubated with monoclonal rabbit anti-GFP IgG fraction (1:200 dilution; Molecular Probes, Eugene, OR). Slides were then blocked for peroxidase with Dakocytomation (S-2001; Dako, Carpinteria, CA) followed by incubation with biotinylated goat anti-rabbit IgG (1:200 dilution; Vector Lab PK-4001, Burlingame, CA). Slides were incubated with avidin–biotin complex (1:200 dilution; Vector Lab, Burlingame, CA) developed with the peroxidase substrate kit (SK-4100; Vector Lab, Burlingame, CA) and lightly stained with Harris hematoxylin. For double immunofluorescence of GFP and vimentin, slides were blocked with horse serum (1:10 dilution) followed by incubation with monoclonal mouse anti-vimentin, Clone V9, M0725 (1:50 dilution; Dako, CA) at 4°C and incubation with secondary antibody Alexa Fluor A555 goat anti-mouse (1:100 dilution; Molecular Probes, Eugene, OR). Slides were blocked with goat serum (1:10 dilution) followed by incubation with monoclonal rabbit anti-GFP IgG fraction (1:200 dilution; Molecular Probes, Eugene, OR) at 4°C and incubation with secondary antibody Alexa Fluor A488 (1:200 dilution; Molecular probes, Eugene, OR). Sections were coverslipped with 4',6'-diamidino-2-phenylindole (Molecular Probes, Eugene, OR), visualized under the microscope (Leica, DMRBE) to analyze the distribution of GFP and the colocalization of GFP and vimentin (Iplab, Scientific Imaging Software, BD Biosciences Bioimaging, Rockville, MD). Double staining for GFP (immunoperoxidase) and SP-B (immunofluorescence) was performed using the techniques described above. For SP-B, slides were incubated with primary antibody (1:200 dilution, Chemicon,

Temecula, CA) followed by incubation with secondary antibody Alexa Fluor A488 goat anti-rabbit (1:100 dilution, Molecular Probes, Eugene, OR). Bright light microscopic and fluorescent images were then merged to produce the images seen in **Figure 4c** and **d**.

Real-time PCR analysis. Samples from the injected lungs were collected at E16.5, E18.5, E21.5, and P7. Extrapulmonary tissues were collected at E21.5 and included the brain, diaphragm, eye, gonads, heart, intestine, kidney, liver, muscle, skin, spleen, stomach, and trachea. All tissues collected for PCR were immediately frozen in liquid nitrogen and stored at -80°C . Genomic DNA was isolated from tissues using the DNeasy Tissue kit (Qiagen, Valencia, CA). Real-time PCR assays were performed on the ABI PRISM 7900s Sequence Detection System. Sequence data were obtained from the GenBank accession nos. U55763 for the cloning vector pEGFP-C1 and NC005111 for *Rattus norvegicus* β -actin region of chromosome 12. The internal probes of both TaqMan systems were labelled at the 5' end with the reporter dye FAM (6-carboxyfluorescein) and at the 3' end with the quencher dye TAMRA (6-carboxytetramethylrhodamine) (IDT, Coralville, IA). The primers and probe for the pEGFP-C1 were as follows: forward 5'-GGGCACAAGCTGGAGTCAACT-3'; reverse 5'-TCTGCTGTGCGCCATGA-3'; probe: 5'-FAM-ACAGCCACAACGTCT-TAMsp-3'. The amplicon size was 61 bp. The β -actin TaqMan system originated an amplicon with 92 bp and consisted of primers and probe as follows: forward 5'-GTATTCCTTTCTCTACAGATCATG-3'; reverse 5'-CCAGAGGCATACAGGGACAAC-3'; probe: 5'-FAM-AGCCATGTACGTAGCCATCCAGGCTG-TAMsp-3'. Amplification conditions were identical for all reactions: 2 min at 50°C, 10 min at 95°C, 40 cycles at 95°C for 15 s, and 60°C for 1 min. The amplification reactions were set in a final volume of 20 μ L, containing 1 \times TaqMan Universal PCR Mastermix (Applied Biosystems), 50 ng of the gDNA sample, 900 nM of each primer, and 250 nM of the respective probe. Negative control was included in all the runs. Standard amplification curve for *eGFP* was made with pEGFP-C1, serially diluted from 2×10^4 to 0.2 copies/ μ L. In all the samples, the calculated pEGFP concentration was normalized for β -actin as internal control. For each experimental group studied, three samples were analyzed in triplicate. Amplification data were analyzed by the sequence detection system software (SDS 1.2 version, Applied Biosystems).

Statistical analysis of data. The results were presented as mean \pm SEM. To ascertain the statistical significance of the differences in the levels of transduction in each tissue at different time points, one-way analysis of variance was performed. Differences between groups were considered to be statistically significant when $P < 0.05$.

ACKNOWLEDGMENTS

We thank Antoneta Radu for her invaluable technical assistance in this study. SG is supported by FCT Grant (SFRH/BD/15260/2004) on behalf of the FCT Grant POCI/SAU-OBS/56428/2004. There are no financial or other relations that could lead to a conflict of interest

SUPPLEMENTARY MATERIAL

Video S1. Fetal lung injections guided by UBM.

Figure S2. Fluorescent and bright light images of the merged images in Figure 4c and d.

REFERENCES

- Porada, CD *et al.* (2005). Gestational age of recipient determines pattern and level of transgene expression following *in utero* retroviral gene transfer. *Mol Ther* **11**: 284–293.
- Zanjani, ED and Anderson, WF (1999). Prospects for *in utero* human gene therapy. *Science* **285**: 2084–2088.
- Waddington, SN, Kennea, NL, Buckley, SM, Gregory, LG, Themis, M and Coutelle, C (2004). Fetal and neonatal gene therapy: benefits and pitfalls. *Gene Ther* **11**: S92–S97.

4. Flake, AW (2003). Stem cell and genetic therapies for the fetus. *Semin Pediatr Surg* **12**: 202-208.
5. Sylvester, KG, Yang, EY, Cass, DL, Crombleholme, TM and Adzick, NS (1997). Fetoscopic gene therapy for congenital lung disease. *J Pediatr Surg* **32**: 964-969.
6. Surbek, DV, Tercanli, S and Holzgreve, W (2000). Transabdominal first trimester embryofetoscopic as a potential approach to early *in utero* stem cell transplantation and gene therapy. *Ultrasound Obstet Gynecol* **15**: 302-307.
7. Larson, JE *et al.* (2000). Gene transfer into the fetal primate: evidence for the secretion of transgene product. *Mol Ther* **2**: 631-639.
8. Buckley, SM *et al.* (2005). Factors influencing adenovirus-mediated airway transduction in fetal mice. *Mol Ther* **12**: 484-492.
9. Holzinger, A, Trapnell, B, Weaver, TE, Whitsett, JA and Iwamoto, HS (1995). Intraamniotic administration of an adenoviral vector for gene transfer to fetal sheep and mouse tissues. *Pediatr Res* **38**: 844-850.
10. Boyle, MP, Enke, RA, Adams, RJ, Guggino, WB and Zeitlin, PL (2001). *In utero* AAV-mediated gene transfer to rabbit pulmonary epithelium. *Mol Ther* **4**: 115-121.
11. Garrett, DJ, Larson, JE, Duna, D, Marrero, L and Cohen, JC (2003). *In utero* recombinant adeno-associated virus gene transfer in mice, rats, and primates. *BMC Biotechnol* **3**: 3-16.
12. Schachtner, S, Buck, C, Bergelson, J and Baldwin, H (1999). Temporally regulated expression patterns following *in utero* adenovirus-mediated gene transfer. *Gene Ther* **6**: 1249-1257.
13. Bouchard, S *et al.* (2003). Long-term transgene expression in cardiac and skeletal muscle following fetal administration of adenoviral or adeno-associated viral vectors in mice. *J Gene Med* **5**: 941-950.
14. Waddington, SN *et al.* (2003). Long-term transgene expression by administration of a lentivirus-based vector to the fetal circulation of immuno-competent mice. *Gene Ther* **10**: 1234-1240.
15. Vincent, MC, Trapnell, BC, Baughman, RP, Wert, SE, Whitsett, JA and Iwamoto, HS (1995). Adenovirus-mediated gene transfer to the respiratory tract of fetal sheep *in utero*. *Hum Gene Ther* **6**: 1019-1028.
16. Peebles, D *et al.* (2004). Widespread and efficient marker gene expression in the airway epithelia of fetal sheep after minimally invasive tracheal application of recombinant adenovirus *in utero*. *Gene Ther* **11**: 70-78.
17. Skarsgard, ED, Huang, L, Reebye, SC, Yeung, AY and Jia, WW (2005). Lentiviral vector-mediated, *in vivo* gene transfer to the tracheobronchial tree in fetal rabbits. *J Pediatr Surg* **40**: 1817-1821.
18. Tarantal, AF *et al.* (2001). Lentiviral vector gene transfer into fetal rhesus monkeys (*Macaca mulatta*): lung-targeting approaches. *Mol Ther* **4**: 614-621.
19. Tarantal, AF *et al.* (2005). Intrapulmonary and intramyocardial gene transfer in rhesus monkeys (*Macaca mulatta*): safety and efficiency of HIV-1-derived lentiviral vectors for fetal gene delivery. *Mol Ther* **12**: 87-98.
20. Turnbull, DH, Bloomfield, TS, Baldwin, HS, Foster, FS and Joyner, AL (1995). Ultrasound backscatter microscope analysis of early mouse embryonic brain development. *Proc Natl Acad Sci USA* **92**: 2239-2243.
21. Foster, FS, Pavlin, CJ, Harasiewicz, KA, Christopher, DA and Turnbull, DH (2000). Advances in ultrasound biomicroscopy. *Ultrasound Med Biol* **26**: 1-27.
22. Hofmann, W *et al.* (1999). Species-specific, postentry barriers to primate immunodeficiency virus infection. *J Virol* **73**: 10020-10028.
23. Romano, G, Michell, P, Pacilio, C and Giordano, A (2000). Latest developments in gene transfer technology: achievements, perspectives, and controversies over therapeutic applications. *Stem Cells* **18**: 19-39.
24. Senoo, M *et al.* (2000). Adenovirus-mediated *in utero* gene transfer in mice and guinea pigs: tissue distribution of recombinant adenovirus determined by quantitative TaqMan-polymerase chain reaction assay. *Mol Genet Metab* **69**: 269-276.
25. Breyer, B *et al.* (2001). Adenoviral vector-mediated gene transfer for human gene therapy. *Curr Gene Ther* **1**: 149-162.
26. Driskell, RA and Engelhardt, JF (2003). Current status of gene therapy for inherited lung diseases. *Annu Rev Physiol* **65**: 585-612.
27. Yang, EY, Cass, DL, Sylvester, KG, Wilson, JM and Adzick, NS (1999). BAPS Prize—1997. Fetal gene therapy: efficacy, toxicity, and immunologic effects of early gestation recombinant adenovirus. British Association of Paediatric Surgeons. *J Pediatr Surg* **34**: 235-241.
28. Naldini, L *et al.* (1996). *In vivo* gene delivery and stable transduction of nondividing cells by a lentiviral vector. *Science* **272**: 263-267.
29. Zufferey, R, Nagy, D, Mandel, RJ, Naldini, L and Trono, D (1997). Multiply attenuated lentiviral vector achieves efficient gene delivery *in vivo*. *Nat Biotech* **15**: 871-875.
30. Sena-Esteves, M, Tebbets, JC, Steffens, S, Crombleholme, T and Flake, AW (2004). Optimized large-scale production of high titer lentivirus vector pseudotypes. *J Virol Methods* **122**: 131-139.
31. Boyd, RL, Francis, EM, Fletcher, MT and Mangos, JA (1984). Pulmonary function of the reserpine and isoproterenol models of cystic fibrosis. *Pediatr Res* **18**: 1028-1031.
32. Muller, RM, Kuipers, GA, Bardon, A, Ceder, O and Roomans, GM (1985). The chronically pilocarpine-treated rat in the study of cystic fibrosis: investigations on submandibular gland and pancreas. *Exp Mol Pathol* **43**: 97-106.
33. Tenbrinck, R *et al.* (1990). Experimentally induced congenital diaphragmatic hernia in rats. *J Pediatr Surg* **25**: 426-429.
34. Olsen, JC (1998). Gene transfer vectors derived from equine infectious anemia virus. *Gene Ther* **5**: 1481-1487.
35. O'Rourke, JP, Hilaragi, H, Urban, K, Patel, M, Olsen, JC and Bunnell, BA (2003). Analysis of gene transfer and expression in skeletal muscle using enhanced EIAV lentivirus vectors. *Mol Ther* **7**: 632-639.
36. Martarano, L, Stephens, R, Rice, N and Derse, D (1994). Equine infectious anemia virus trans-regulatory protein Rev controls viral mRNA stability, accumulation, and alternative splicing. *J Virol* **68**: 3102-3111.
37. Stetor, SR *et al.* (1999). Characterization of (+) strand initiation and termination sequences located at the center of the equine infectious anemia virus genome. *Biochemistry* **38**: 3656-3667.
38. Donello, JE, Loeb, JE and Hope, TJ (1998). Hope Woodchuck hepatitis virus contains a tripartite posttranscriptional regulatory element. *J Virol* **72**: 5085-5092.
39. Davis, A and Wilson, J (1996). Adenovirus vectors. *Curr Protocols Hum Genet*: 12.4.1-12.4.18.
40. Davis, A, Wivel, NA, Palladino, JL, Tao, L and Wilson, JM (2001). Construction of adenoviral vectors. *Mol Biotechnol* **18**: 63-70.
41. Ng, P and Graham, FL (2002). Construction of first-generation adenoviral vectors. *Methods Mol Med* **69**: 389-414.